

## Supplementary information

### Concentration gradient generator using a convective-diffusive balance

Taekyu Kang,\* Jeahyeong Han, and Ki Sung Lee

*Department of Mechanical Science and Engineering, University of Illinois at Urbana-Champaign, IL 61801-2906, USA.*

Author to whom correspondence should be addressed, taekang@uiuc.edu

### Micro-fabrication procedures

A 100 mm diameter, 400  $\mu\text{m}$  thickness silicon wafer was patterned with a AZ 4620 photoresist and subsequently etched through 325  $\mu\text{m}$  deep by using Bosch process in a deep reaction ion etching system (Plamsa-Therm SLR 770). This process created the inlet and the outlet channels with the dimensions of 1000  $\mu\text{m}$  x 325  $\mu\text{m}$  and 50  $\mu\text{m}$  x 325  $\mu\text{m}$ , respectively. After the removal of the PR with a 400T stripper, the silicon wafer and a coverglass were cleaned in SC-1 solution. The custom-made epoxy is spin-coated onto a PDMS round carrier substrate, and the adhesive is transferred to the silicon surface. Following this step, the silicon was pressed with a Teflon ball from the top of the coverglass at 110°C, and cured at 140°C for 10 minutes on a hotplate. The package to accommodate this device was manufactured by using a stereo lithography (SLA) machine.

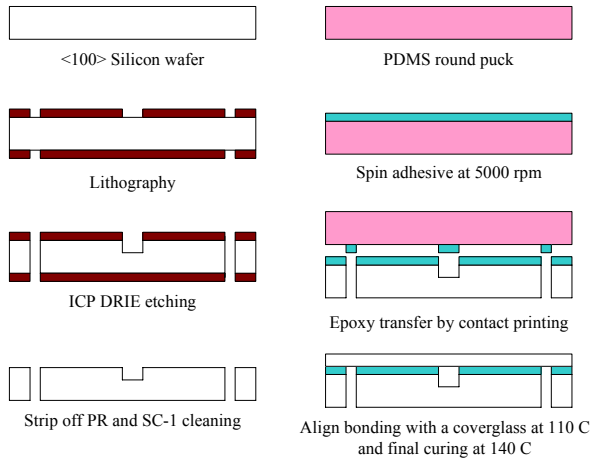


**Figure S1** Micro-fabrication process

### Verification of concentration uniformity in the y-axis (-200 $\mu\text{m}$ to 200 $\mu\text{m}$ )

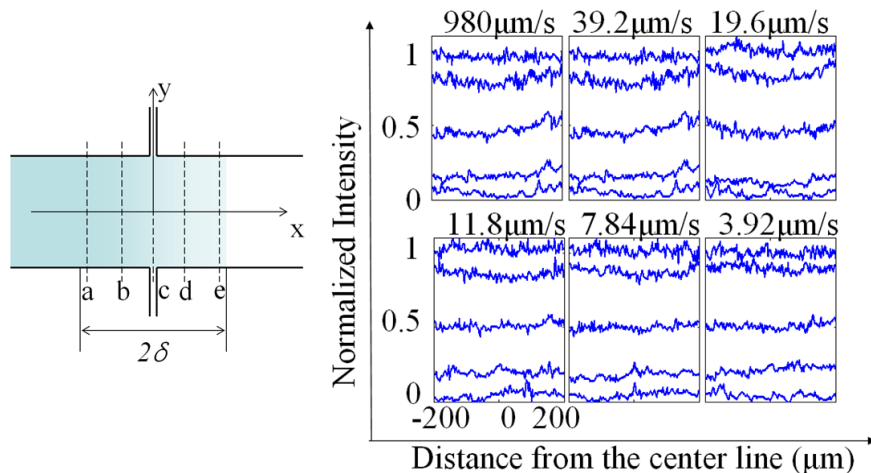


**Figure S2** Normalized fluorescence intensity plots along the equally distributed lines, a, b, c, d, and e within  $2\delta$  and from -200  $\mu\text{m}$  to 200  $\mu\text{m}$  in the y-direction.

### Determination of $K$ (1/sec)

In order to make comparison between experimental and theoretical concentration gradient profiles, we first were required to define a method to calculate a strain rate. For the length scale for the strain rate (=velocity/length), it was reasonable to take the distance between a stagnation plane and a location where convective speeds started to decrease. To accurately pinpoint the locations at which flow speeds started to decrease, a commercial CFD package, FLUENT 6.3.26, was employed to simulate our experiments and the results of the flow speeds along the x-axis were shown in Fig. S3. Since the normalized velocity profiles were identified to have approximate similarity irrespective of flow rates, the single location ( $x=-925$  and  $925 \mu\text{m}$ ) at which the speed reduced to 99.9% of its maximum value was chosen as the length scale to calculate the strain rate. The initial increase of the flow speeds in Fig. S3 was the indication for the flow to be fully developed.

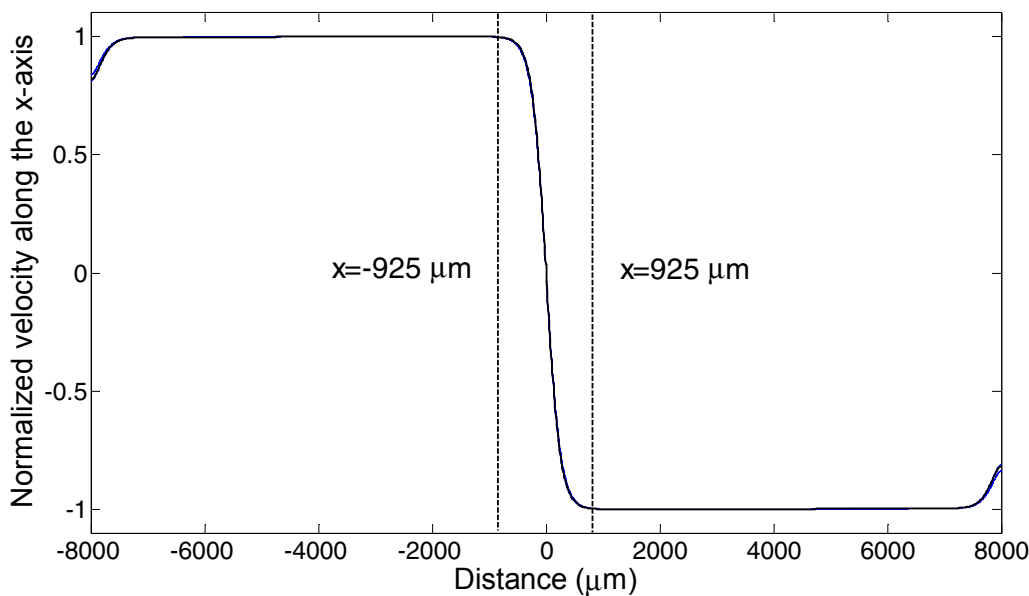


**Figure S3** Normalized velocity along the x-axis (calculation results using FLUENT 6.3.26).

### Shear stress distribution

Shear stress distribution was calculated using FLUENT 6.3.26, which indicated that the scale of the shear stresses were much below physiologically relevant shear stress levels ( $\sim 10^{-3}$  dyne/cm $^2$ ).

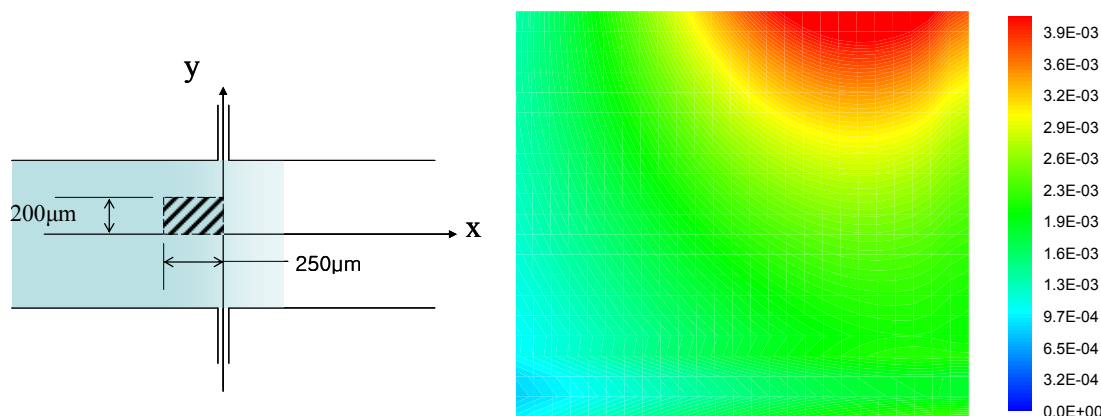


**Figure S4** Shear stress (dyne/cm $^2$ ) distribution in the quadrant region under a convective speed of 39.2 μm/s (FLUENT 6.3.26).

### Effects of the outlet channel size on concentration distribution

To investigate the effects of the outlet channel size on concentration distribution, two different outlet widths ( $50\text{ }\mu\text{m}$ ,  $200\text{ }\mu\text{m}$ ) with a convective speed of  $39.2\text{ }\mu\text{m/s}$  were simulated. As shown in Fig. S5, the results can be reasonably assumed to be identical with the region of interest.

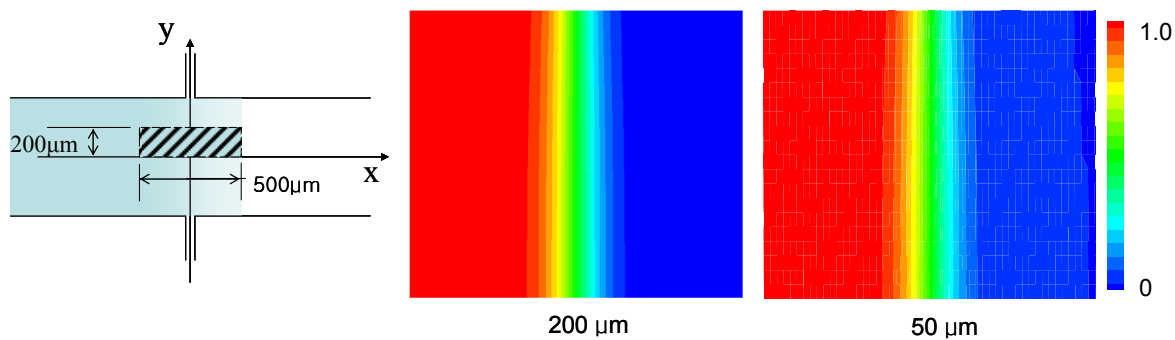


**Figure S5** Normalized Rhodamine 6G concentration distribution in the upper half of the region of interest under a convective speed of  $39.2\text{ }\mu\text{m/s}$  (FLUENT 6.3.26).